X-932-74-99
PREPRINT

AN ANALYTIC METHOD TO ACCOUNT FOR DRAG IN THE VINTI SATELLITE THEORY

J. S. WATSON
G. D. MISTRETTA
N. L. BONAVITO

APRIL 1974

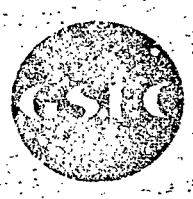

GODDARD SPACE FLIGHT CENTER
GREENBELT, MARYLAND

AN ANALYTIC METHOD TO ACCOUNT FOR DRAG IN THE VINTI SATELLITE THEORY

J. S. Watson

G. D. Mistretta

N. L. Bonavito

April 1974

GODDARD SPACE FLIGHT CENTER

Greenbelt, Maryland

AN ANALYTIC METHOD TO ACCOUNT FOR DRAG IN THE VINTI SATELLITE THEORY

J. S. Watson
G. D. Mistretta
N. L. Bonavito

ABSTRACT

In order to retain separability in the Vinti theory of earth satellite motion when a non-conservative force such as air drag is considered, a set of variational equations for the orbital elements are introduced, and expressed as functions of the transverse, radial, and normal components of the nonconservative forces acting on the system. In this approach, the Hamiltonian is preserved in form, and remains the total energy, but the initial or boundary conditions and hence the Jacobi constants of the motion advance with time through the variational equations. In particular, the atmospheric density profile is written as a 'fitted' exponential function of the eccentric anomaly, which adheres to tabular data at all altitudes and simultaneously reduces the variational equations to indefinite integrals with closed form evaluations, whose limits are in terms of the eccentric anomaly. The values of the limits for any arbitrary time interval are obtained from the Vinti program.

Results of this technique for the case of the intense air drag satellites San Marco-2 and Air Force Cannonball are given. These results indicate that the satellite ephemerides produced by this theory in conjunction with the Vinti program are of very high accuracy. In addition, since the program is entirely analytic, several months of ephemerides can be obtained within a few seconds of computer time.

CONTENTS

INTRODUCTION

Vinti (Reference 1) has shown that if a satellite orbit is described by means of osculating Jacobi α's and β's of a separable problem, then a perturbing force $\bar{F}$ makes them vary according to

$$\dot{\alpha}_K = \bar{F} \cdot \partial \bar{r} / \partial \beta_K, \qquad \dot{\beta}_K = - \bar{F} \cdot \partial \bar{r} / \partial \alpha_K, \qquad (K = 1, 2, 3).$$

Here $\bar{r}$ is the position vector of the satellite and $\bar{F}$ is any perturbing force, conservative or non-conservative. If $\bar{F}$ is the force of air drag, the interaction of drag with oblateness makes it desirable to obtain variations to the order drag $\times J_2$, where J_2 is the coefficient of the second zonal harmonic of the Earth's gravitational potential. The physical reason for carrying these derivatives through order J_2 is the strong variation of drag with perigee height. In the present paper, we have been able to account for this effect without introducing the J_2 terms into $\partial \bar{r} / \partial \beta_K$ and $\partial \bar{r} / \partial \alpha_K$. The logic behind our approach requires a rather careful exposition which we shall go into in detail in Section I. The essence of the method is that for a given time interval, one always does both a drag free calculation, and an oblateness free calculation with drag, and that these two calculations are done in a self-consistent iterative manner such that the mean orbital elements never go far astray. The appropriate criterion, to make sure that the drag-oblateness interaction is being properly accounted for, is that the perigee height corresponding to initial and final orbital elements of a given interval shall not change by more than some predetermined amount.

The complexity of those papers which attempt to handle the oblateness-drag interaction in a straight forward manner (References 2, 3) illustrates the desirability of finding a new approach. That is the purpose of this paper.

I. STATEMENT OF THE PROBLEM

In this paper we consider the motion of an artificial Earth satellite in the presence of air drag and the Earth's gravitational potential. In contrast to the classical methods of numerical integration, our approach will be to present a quadrature algorithm employing analytical expressions for the variation of orbital elements produced by air drag. These expressions are well-defined over expanded subintervals of the solution, and produce accurate agreement with profiles of tabular density. This procedure then allows a flexibility in the selection of end points of the subintervals, which in turn insures a minimum error bound on the required analytical function. For convenience we shall henceforth refer to the algorithm as the BMW (Bonavito-Mistretta-Watson) aerodynamic method. In this method the effect of oblateness is accounted for by the Vinti Spheroidal Theory (Reference 4). The changes due to atmospheric resistance for a non-rotating sphere are accounted for by the solutions of the variational equations without oblateness (Reference 5).

Normally, one would wish to represent the variation of atmospheric density by an exponential whose power is a function of the difference between the satellite height and the altitude at a predetermined density (Reference 6). Such a representation is usually valid only in a neighborhood of this boundary value. The neighborhood or region over which this density representation is in agreement with tabular data such as provided by the U. S. Standard Atmosphere Supplements, 1966, (Reference 7), is one in which the density scale height is observed to vary in an approximate linear fashion. Throughout our calculations a set of such regions is chosen to meet this requirement. In addition, the initial or boundary value of the atmospheric density for each of these regions is also

supplied by the Supplements. Such a representation for atmospheric density would,except under special conditions, exclude closed form integration of the variational equations. To avoid this difficulty, we approximate the atmospheric density variation by an expression which is made to adhere closely to the numerical values of the aforementioned model. By adjusting or advancing boundary conditions over several selected arcs or layers of atmospheric density, we produce a profile that closely agrees with the tabulated data for all heights. The degree to which our results compare with tabular values (Spring-Fall model, 1100°K exospheric temperature) from the U. S. Standard Atmospheric Supplements, 1966, is shown in Table I. Between the heights of 205 kilometers and 650 kilometers, the discrepancy is less than two percent. From symmetry considerations, these sets of boundary conditions for one representation can be determined during the first half revolution of an orbit. These density variation profiles then are held fixed until such time as the perigee height changes by some predetermined amount. At this point the boundary conditions are redetermined over the first half revolution away from perigee, corresponding to a chosen epoch. This again produces a total density profile that is in close agreement with the values from the Supplement tables. Experience indicates that given a criterion of one kilometer change in perigee, this redetermination is not necessary for nearly two months in the cases of the San Marco-2 and Cannonball satellites, but becomes more frequent near the end of the lifetime of each spacecraft.

In our final expressions for these variations, rotation of the atmosphere is accounted for while an oblate atmosphere is considered in a partial fashion by including the oblateness parameter in the exponential term of the density

variation. Although the variational equations do not contain the effects of oblateness explicitly, the interaction between oblateness and drag is accounted for implicitly during the computational procedure in the following manner (See Figure 5).

1. From the initial conditions calculate the Izsak elements of the Vinti Spheroidal Theory corresponding to that epoch.

2. With these, together with tabular data or air density, obtain the density variation profiles and corresponding values for changes in the elements arising from air drag for those altitudes during the first half revolution past perigee and beyond epoch, corresponding to these density profiles.

3. For any desired time interval, calculate using oblateness only (without drag) $\bar{r}$ and $\dot{\bar{r}}$ and the value of the eccentric anomaly E_u at the end of this interval from the initial given set of Vinti or Izsak elements.

4. For this same time interval, calculate from drag only (without oblateness) the total change in the original or given set of Vinti elements, using the value of the eccentric anomaly obtained in step (3) as the upper limit in the analytical expressions for these changes in the elements arising from drag. The total change in the elements from epoch to this time, produced by drag only, are obtained by multiplying the revolutions to this point in the orbit by the sum of the individual (analytically expressed) corrections or changes to the elements obtained in the first half revolution.

5. Add these changes arising from drag of step (4) to the epoch values of the Vinti elements.

6. For the same time interval, repeat step (3) with the new elements obtained in step (5).

7. Compare the last two values of eccentric anomaly. If their difference is less than some arbitrary preassigned small positive number ϵ, then the differences between the original noniterated set of elements $\alpha_i^{(0)}$, $\beta_i^{(0)}$ (i = 1,2,3), and the iterated set $\alpha_i^{(n)}\beta_i^{(n)}$ approaches a constant. That is, when

$$\left| \frac{E_u^{(n)} - E_u^{(n-1)}}{E_u^{(n)}} \right| < \epsilon,$$

then,

$$\Delta\alpha = (\alpha^{(0)} - \alpha^{(n)}) = H(\alpha^{(n-1)}, E_u^{(n-1)}) \rightarrow \text{constant}.$$

Similarly,

$$\Delta\beta = (\beta^{(0)} - \beta^{(n)}) = G(\beta^{(n-1)}, E_u^{(n-1)}) \rightarrow \text{constant}$$

where (n) is the iteration number. Note that the functional representation of the variational equations solution on the right hand side contains the previous iterated values of the elements and the eccentric anomaly, ($\alpha^{(n-1)}$, $\beta^{(n-1)}$, $E_u^{(n-1)}$).

8. If the above criterion on the eccentric anomaly upper limit is met, then we accept the $\alpha_i^{(n)}$, $\beta_i^{(n)}$ as the new Vinti elements that describe the orbit from the original epoch to the end of the given time interval.

9. If the criterion is not met, repeat steps (3) through (7) always utilizing the iterated values of the Vinti elements in the calculation of step (3) until such time as

$$\left| \frac{E_u^{(n)} - E_u^{(n-1)}}{E_u^{(n)}} \right| < \epsilon.$$

In functional terms, if by $\bar{x}$ we denote the elements of the Vinti Satellite Theory and $f(\bar{x}, t)$ represents the Vinti Spheroidal Method (oblateness only) solution which for a given time interval yields a value of the eccentric anomaly E_u corresponding to a time t at the end of that interval, and $g[\bar{x}, f(\bar{x},t)]$ represents the correction arising from drag plus the oblateness calculation; then for a fixed value of time t, the above algorithm is an iterative solution for $\bar{x}$ using the equation

$$f(\bar{x},\ t) = f(g[\bar{x},\ f(\bar{x},\ t)],\ t)$$

in a self-consistent method. Thus, for a fixed time interval

$$(\alpha^0,\ \beta^0)_{\text{oblateness}} \rightarrow E_U^{(1)} \rightarrow (\Delta\alpha^{(1)},\ \Delta\beta^{(1)})_{\text{drag}} \rightarrow (\alpha^{(1)},\ \beta^{(1)})_{\text{oblateness}}$$

$$\rightarrow E_U^{(2)} \rightarrow (\Delta\alpha^{(2)},\ \Delta\beta^{(2)})_{\text{drag}} \rightarrow \ldots \rightarrow (\alpha^{(n-1)},\ \beta^{(n-1)})_{\text{oblateness}}$$

$$\rightarrow E_U^{(n)} \rightarrow (\Delta\alpha^{(n)},\ \Delta\beta^{(n)})_{\text{drag}} \rightarrow (\alpha^{(n)},\ \beta^{(n)}).$$

This algorithm converges when

$$\left| \frac{E_U^{(n)} - E_U^{(n-1)}}{E_U^{(n)}} \right| < \epsilon.$$

II. AERODYNAMIC DRAG VARIATIONAL EQUATIONS

From Sterne (Reference 5), the equations for variations of the orbital elements due to air drag and without oblateness are given by

$$
\begin{aligned}
\frac{da}{dt} &= 2\left(\frac{a^3}{\mu}\right)^{1/2}\frac{1}{\sqrt{1-e^2}}\left[Re\sin v + T(1+e\cos v)\right] \\
\frac{de}{dt} &= \left(\frac{a}{\mu}\right)^{1/2}\sqrt{1-e^2}\left[R\sin v + T(\cos v + \cos E)\right] \\
\frac{di}{dt} &= W\left(\frac{r\cos\psi}{na^2\sqrt{1-e^2}}\right) \\
\frac{d\omega}{dt} &= -R\left(\frac{\sqrt{1-e^2}\cos v}{nae}\right) + T\left(\frac{\sqrt{1-e^2}\left(1+\frac{r}{p}\right)\sin v}{nae}\right) - W\left(\frac{r\cos i\sin\psi}{na^2\sqrt{1-e^2}\sin i}\right) \\
\frac{d\Omega}{dt} &= W\left(\frac{r\sin\psi}{na^2\sqrt{1-e^2}\sin i}\right) \\
\frac{dM}{dt} &= n + R\left(\frac{(1-e^2)}{nae}\cos v - \frac{2r}{na^2}\right) - T\left(\frac{(1-e^2)\left(1+\frac{r}{p}\right)\sin v}{nae}\right).
\end{aligned}
\tag{1}
$$

Here ψ is the argument of latitude, $r = a(1-e\cos E)$, $p = a(1-e^2)$, and $n = \mu^{1/2}\, a^{-3/2}$, where μ is the product of the gravitational constant and the sum of the masses in the two body problem. E and v are the eccentric and true anomaly respectively and i is the inclination. The drag perturbing force is resolved into the following components:

R is in the direction of the position vector from the force center to the satellite.

T is perpendicular to R, lies in the orbital plane, and is positive in the direction of motion.

W is mutually perpendicular to R and T and completes a right handed set of component directions.

In terms of the eccentric anomaly, these are given by

$$R = -\frac{1}{2} C_D \frac{A}{m} ae\rho V \sin E \frac{dE}{dt}$$

$$T = -\frac{1}{2} C_D \frac{A}{m} (1 - e^2)^{1/2} a\rho V \left[1 - d \frac{(1 - e \cos E)^2}{(1 - e^2)}\right] \frac{dE}{dt} \qquad (2)$$

$$W = -\frac{1}{2} C_D \frac{A}{m} a\rho\omega_s V\mu^{-1/2} a^{3/2}$$

$$\times (1 - e \cos E)^2 \sqrt{S} \cos\psi \frac{dE}{dt}.$$

Here, ω_s is the angular velocity of rotation of the Earth, ρ is the atmospheric density, A is the projected area of the satellite, m is the mass of the satellite, and C_D is a drag parameter. S is a parameter related to the orbital inclination and is given by

$$S = \sin^2 i. \qquad (3)$$

The velocity of the satellite relative to the atmosphere can be written in vector notation as

$$\bar{V} = \dot{\bar{r}} - \bar{\omega}_s \times \bar{r}.$$

Neglecting the term of order ω_s^2 in the magnitude of $\bar{V}$ to be employed in (2), one obtains the expression given by Sterne to be

$$V = \left(\frac{\mu}{a}\right)^{1/2} (1 + e \cos E)^{-1/2} (1 - e \cos E)^{-1/2} [(1 + e \cos E) - d(1 + e \cos E)]$$

where

$$d = \omega_s \mu^{-1/2} a^{3/2} (1 - e^2)^{1/2} (1 - S)^{1/2} \operatorname{sgn} \alpha_3$$

where $\operatorname{sgn} \alpha_3 = +1$ or -1 according to whether the orbit is direct or retrograde. From (3) above we have

$$\frac{dS}{dt} = 2 \sin i \cos i \frac{di}{dt},$$

or

$$\frac{dS}{dt} = 2 \sqrt{S} \sqrt{1 - S} \frac{di}{dt}.$$

Inserting di/dt from (1), we can then write the variation of the inclination parameter as

$$\frac{dS}{dt} = \frac{2 \sqrt{S(1 - S)}\, rW \cos \psi}{\sqrt{\mu a}\, \sqrt{1 - e^2}}.$$

Let us now write the right ascension of the ascending node and the argument of perigee as β_3 and β_2 respectively. In addition, the mean anomaly is related to the time of perigee passage β_1 by $M = n(t + \beta_1)$. Differentiating, we have that

$$\frac{d\beta_1}{dt} = \frac{1}{n} \left[\frac{dM}{dt} - (t + \beta_1) \frac{dn}{dt} - n \right]$$

where

$$\frac{dn}{dt} = -\frac{3}{2} \mu^{1/2} a^{-5/2} \frac{da}{dt}.$$

Using the above results, together with (2), the solutions of the variational equations due to air drag without oblateness are given from (1) by

$$\Delta a = -\frac{C_D A}{m}\, a^2 \int_{E_1}^{E_2} \rho\{(1 - e\cos E)^{-1/2}\,(1 + e\cos E)^{-1/2}\,[(1 + e\cos E)$$

$$- d(1 - e\cos E)]^2\}\, dE$$

$$\Delta e = -\frac{C_D A}{m}\, a(1 - e^2) \int_{E_1}^{E_2} \rho\left(\frac{1 + e\cos E}{1 - e\cos E}\right)^{-1/2} \left[1 - \frac{d(1 - e\cos E)}{(1 + e\cos E)}\right]$$

$$\times \left[\cos E - \frac{d}{2}\,(1 - e^2)^{-1}\,(1 - e\cos E)\,(2\cos E - e - e^2\cos^2 E\right]\, dE$$

$$\Delta S = -\frac{C_D A}{m}\,\omega_s \frac{a}{n}(1 - e^2)^{-1/2}\, S \quad \sqrt{1 - S} \int_{E_1}^{E_2} \rho(1 + e\cos E)^{-1/2}$$

$$\times (1 - e\cos E)^{5/2}\cos^2\psi[(1 + e\cos) - d(1 - e\cos E)]\, dE$$

(4)

$$\Delta\beta_3 = -\frac{1}{2}\, C_D \frac{A}{m}\,\mu^{-1/2}\, a^{5/2}\,\omega_s (1 - e^2)^{-1/2} \int_{E_1}^{E_2} \rho \sin\psi\cos\psi$$

$$\times (1 + e\cos E)^{-1/2}\,(1 - e\cos E)^{5/2}\,[(1 + e\cos E) - d(1 - e\cos E)]\, dE$$

$$\Delta\beta_2 = -\frac{1}{2} C_D \frac{A}{m} a e^{-1}(1 - e^2)^{-1/2} \int_{E_1}^{E_2} \rho\Big\{-e\sin\psi\cos\psi\,\frac{\omega_s}{n}\,\sqrt{1 - S}\,\operatorname{sgn}\alpha_3$$

$$\times (1 + e\cos E)^{-1/2}\,(1 - e\cos E)^{-5/2}\,[(1 + e\cos E) - d(1 - e\cos E)]$$

$$+ 2(1 + e\cos E)^{-1/2}\,(1 - e\cos E)^{-1/2}\sin E[(1 + e\cos E) - d(1 - e\cos E)]$$

$$\times \left[1 - e^2 - \frac{d}{2}\,(1 - e\cos E)\,(2 - e^2 - e\cos E)\right]\Big\}\, dE$$

and

$$\Delta\beta_1 = \frac{3}{2}\frac{\Delta a}{a}(t + \beta_1) - \frac{\sqrt{1-e^2}}{n}(\Delta\beta_2 + \sqrt{1-S}\,\Delta\beta_3 \operatorname{sgn}\alpha_3)$$

$$+ \frac{C_D A}{m}\frac{ae}{n}\int_{E_1}^{E_2} \rho(1 - e\cos E)^{1/2}(1 + e\cos E)^{-1/2}$$

$$\times [(1 + e\cos E) - d(1 - e\cos E)]\sin E dE.$$

Here E_1 and E_2 are the values of the eccentric anomaly at arbitrary times t_1 and t_2 respectively and the time t is usually taken to be the time of epoch.

The solution of (4) will be considered in Section IV after describing the form of ρ in Section III.

III. ATMOSPHERIC DENSITY REPRESENTATION

At this point we consider the expression for atmospheric density variation given by King-Hele (Reference 6). An expression for the atmospheric density as a function of the eccentric anomaly is given by

$$\rho = \rho_p\{1 + b(r - r_p)^2\}\exp\left(-\frac{r - r_p}{H_p}\right)$$

$$= \rho_p\{1 + bx^2(1 - \cos E)^2\}\exp\left\{-\frac{x}{H_p}(1 - \cos E)\right\} \qquad (5)$$

where $x = ae$, H_p = density scale height at perigee which in equation (5) is assumed to vary linearly with the perigee height.

Let us now write equation (5) in a more general form so as to represent the atmospheric density variation over any interval within the orbit in which

the boundary conditions are known. A generalization of (5) is desirable for our purposes to insure that the resultant analytic atmospheric model rigidly adheres to a tabular set of densities at all altitudes. To obtain this generalization, let the subscripts L and U refer to a lower and upper point of an interval respectively. This interval $[E_L, E_U]$ is judiciously chosen (by a method discussed later in this section) and allows either

$$0 \le E_L \le \pi \quad \text{and} \quad 0 \le E_U \le \pi$$

or

$$\pi \le E_L \le 2\pi \quad \text{and} \quad \pi \le E_U \le 2\pi.$$

Letting

$$r_L = a(1 - e \cos E_L), \qquad r_U = a(1 - e \cos E_U),$$

and

$$r_{min} = \min(r_L, r_U), \qquad r_{max} = \max(r_L, r_U),$$

permits ρ to be given by an expression of the type of equation (5) over the restricted domain $[E_L, E_U]$ by

$$\rho(r) = \rho_L \{1 + b(L, U)\,(r - r_{min})^2\} \exp\left(-\frac{r - r_{min}}{H_L}\right) \qquad r_{min} \le r \le r_{max}$$

or

$$\rho(E) = \rho_L \{1 + b(L,U)\, x^2 (\cos E_L - \cos E)^2\} \exp\left\{-\frac{x}{H_L}(\cos E_L - \cos E)\right\}, \quad E_L \le E \le E_U \qquad (6)$$

where ρ_L and H_L are available from density tables, E_L and E_U are available from the orbit theory (as are r_L and r_U), and b(L,U) is derivable from (6) by setting $\rho(E_U) = \rho_U$ which yields $b(L, U) = b(L, U; \rho_L, \rho_U, r_L, r_U, H_L)$.

If equation (6) above is substituted into (4) and the resulting expressions are expanded in powers of the eccentricity e, this yields terms of the form

$$\int_{E_1}^{E_2} \sin^n E \cos^m E \exp\{-(x/H_L)(\cos E_L - \cos E)\}\, dE$$

where $m \geq 0$, $n \geq 0$, and H_L is held constant over the range of a subinterval of integration and x is held constant over the entire range of integration. For the case $n = 0$, this expression can be evaluated in terms of Bessel functions for the limits $(0,\pi)$. The parameter n, however, does assume the value zero; and, in addition, it is desirable to alter the form of the integrand so as to insure that the expression under the integral sign is integrable over any interval while simultaneously maintaining its theoretical physical content. In short, the variational equations cannot be solved by the Fundamental Theorem of Calculus since an antiderivative of $\sin^n E \cos^m E \exp\{-(x/H_L)(\cos E_L - \cos E)\}$, $(n \neq 1)$, is not expressible in terms of elementary functions.

To achieve this purpose let us now consider the following: rewrite the expression for atmospheric density (5) as

$$\rho(E) = \rho_L [1 + b(L, U) x^2 (\cos E_L - \cos E)^2]\, b_1(E) \exp[b_2(E) \cdot E]$$

$$E_L \leq E \leq E_U \qquad (7)$$

where $b_1(E)$, $b_2(E)$ are arbitrary functions of E which will be chosen to preserve closed form integrability of the variational equations (4) while retaining near complete numerical agreement with the exponential term of King-Hele's expression for $\rho(E)$.

The selection of the two functions $b_1(E)$, $b_2(E)$ between an upper limit of integration E_2 and a lower limit E_1 will be made in the following manner.

Consider the interval $[E_1^*, E_2^*]$ subdivided into a collection of n nonoverlapping subintervals I_ℓ, ($\ell = 1, 2, \ldots, n$), defined by the partitioning

$$E_1^* = x_0 < x_1 < \ldots < x_{n-1} < x_n = E_2^*.$$

For any subinterval $I_\ell = [x_{\ell-1}, x_\ell]$, define

$$\begin{aligned} b_1(E) &= c_\ell \\ b_2(E) &= d_\ell \end{aligned} \qquad \text{for} \quad x_{\ell-1} \le E \le x_\ell$$

where c_ℓ, d_ℓ are constants. The determination of c_ℓ, d_ℓ will be accomplished by applying the technique of classical weighted least squares. In this manner the definition of $b_1(E)$ and $b_2(E)$ over the domain $[E_1^*, E_2^*]$ are the step functions

$$\begin{aligned} b_1(E) &= c_1 \quad && x_0 \le E \le x_1 \\ &= c_2 && x_1 \le E \le x_2 \\ &\vdots && \vdots \\ &= c_n && x_{n-1} \le E \le x_n \end{aligned}$$

$$\begin{aligned} b_2(E) &= d_1 \quad && x_0 \le E \le x_1 \\ &= d_2 && x_1 \le E \le x_2 \\ &\vdots && \vdots \\ &= d_n && x_{n-1} \le E \le x_n. \end{aligned}$$

Consider observational data Y_i generated within I_ℓ by repeated evaluation of the function

$$h(E_i) = \exp[-\mathcal{A}(\cos E_L - \cos E_i)]$$

where $\mathcal{A} = x/H_L$ and $x_{\ell-1} \leq E_i \leq x_\ell$. To define the pseudo-regression situation governing our estimation problem, consider the implicitly linear, exponential model

$$Y_i = \beta_1 \epsilon_i \exp(\beta_2 E_i) \qquad i = 1, 2, \cdots, m \tag{8}$$

relating the independent variable E and the dependent or response variable Y that, unlike the general regression response variable, displays no random variability. Hence, the random variables ϵ_i denoting the dispersion characteristics of Y_i about the theoretical regression line become meaningless in the curve fitting analysis. That is, the random variables ϵ_i are degenerate in the sense that their probability density functions $p(\epsilon_i)$ are given by

$$\begin{aligned} p(\epsilon_i) &= 1 \qquad \epsilon_i = B_i \\ &= 0 \qquad \text{otherwise} \end{aligned}$$

where B_i can be considered a "fitting bias" at $E = E_i$ since

$$E(\epsilon_i) = B_i \qquad Var(\epsilon_i) = 0.$$

While all practical statistical properties of the regression analysis become lost, the technique is not degraded as a numerical tool for approximating with great precision complex functional forms over restricted regions with relatively simple functions.

To display the implicit linear form of (8), we take the natural logarithm of both sides of (8) and obtain the equivalent form

$$\ln Y_i = \ln \beta_1 + \beta_2 E_i + \ln \epsilon_i$$

or

$$Y_i' = \beta_1' + \beta_2 E_i + \epsilon_i' \quad (i = 1, 2, \cdots, m).$$

If nonnegative weights $\omega_1, \omega_2, \ldots, \omega_m$ are available and y_i' are evaluated from $y_i' = \ln h(E_i) = -Q(\cos x_{\ell-1} - \cos E_i)$, then the well known result

$$b_1' = \left(\sum_1^m \omega_i\right)^{-1} \sum_1^m \omega_i y_i' - b_2 \left(\sum_1^m \omega_i\right)^{-1} \sum_1^m \omega_i E_i$$

$$b_2 = \frac{\sum_1^m \omega_i y_i' E_i - \left(\sum_1^m \omega_i\right)^{-1} \left(\sum_1^m \omega_i y_i'\right) \left(\sum_1^m \omega_i E_i\right)}{\sum_1^m \omega_i E_i^2 - \left(\sum_1^m \omega_i\right)^{-1} \left(\sum_1^m \omega_i E_i\right)^2}$$

are the values of β_1', β_2 that minimize the weighted sum of squares

$$\sum_1^m \omega_i \epsilon_i'^2 = \sum_1^m \omega_i (y_i' - \beta_1' - \beta_2 E_i)^2.$$

Thus, $b_1 = \exp(b_1')$ and b_2 are the classical weighted least squares estimated of β_1, β_2 respectively.

The selection of the mesh points over an interval of integration $[E_1^*, E_2^*]$ is obtained through an automated search approach utilizing the weighted least squares process previously described. This technique selects subintervals of maximum size while retaining a user selected error tolerance between the true and predicted function.

Furthermore, if one sets $E_1^* = 0$, $E_2^* = \pi$, and derives a set of coefficients for the n selected subintervals in the manner previously defined, the functions

h(E) and ρ (E) will have been fitted for all values of E over which x has been assumed constant. This is true since h(E) is a periodic function with period 2π and in the fundamental period (0, 2π) is symmetrically distributed about the axis of symmetry $E = \pi$.

With the use of more general expression for density (ρ), the variational equations (4) integrated between E_1^* and E_2^* where $0 < E_1^* < E_2^* < \pi$, take on the following general functional form

$$\Delta q_k = \sum_{j=0}^{n-1} \int_{x_j}^{x_{j+1}} \{t_{j+1} \exp(d_{j+1} E)\} \, dG_k(E) \quad (k = 1, 2, \cdots, 6)$$

where $dG_k(E) = g_k(\sin E, \cos E)\, dE$. Having fitted h(E) from $(0 - \pi)$, the integration of the variational equations between any two arbitrary limits $E_1^* \geq 0$, $E_2^* > E_1^*$, takes the general functional form

$$\begin{aligned}
\Delta q_k = & \sum_{j=0}^{n-1} m_{j+1} \int_{x_j}^{x_{j+1}} \{t_{j+1} \exp [d_{j+1} E\} \, dG_k(E) \\
& + \sum_{j=0}^{n-1} m_{2n-j} \int_{2\pi - x_{j+1}}^{2\pi - x_j} \{t'_{2n-j} \exp [d'_{2n-j} E]\} \, dG_k(E) \\
& + \int_{x_\xi}^{E_2^* \bmod 2\pi} t_\xi^* \exp(d_\xi^* E) \, dG_k(E) \\
& + \int_{E_1^* \bmod 2\pi}^{x_\eta} t_\eta^* \exp(d_\eta^* E) \, dG_k(E) \quad (k = 1, 2, \cdots, 6)
\end{aligned} \tag{9}$$

where m_ℓ, (ℓ = 1, 2, . . . , 2n), are nonnegative integers; t_j, t_k', d_k' (j = 1, 2, . . . , n), (k = n + 1, n + 2, . . . , 2n) are functions of c_j, d_j; ξ is an integer between 0 and 2n - 2; η is an integer between 1 and 2n - 1; the grid points $x_{n+1}, x_{n+2}, \ldots, x_{2n}$ are defined from $x_0, x_1, \ldots, x_n$; and (t*, t*) may be either (t_ξ, t_ξ), (t_ξ', t_η), (t_ξ, t_η'), (t_ξ', t_η') depending upon the values $E_1^* \bmod 2\pi$, $E_2^* \bmod 2\pi$. The logical structure of (13) and the determination of the above parameters is too lengthy to be given here but is presented in Appendix for completeness. It must be emphasized that (13) is general for all computations, but is valid only while x is assumed constant, whereby a new fit is obtained and new constants are determined to integrate (4) by the general form (9).

Using these results we can now solve the density expression for the value of b within each of the selected or fitted intervals from the expression

$$b(L, U) = \frac{-\rho_L + \rho_U \exp[(r_U - r_L)/H_L]}{\rho_L (r_U - r_L)^2}$$

where the subscripts U and L still refer to the upper and lower points of an interval. For example, ρ_L is that value of density at the initial point of the interval which is known from the tables, and the corresponding density scale height H_L can then be computed. The end point r_U is known as a function of E_2. Therefore H_L is also 'advanced' in a similar fashion as ρ_L during the fitting of the exponential. The above method of fitting King-Hele's expression over several intervals of an orbit is sufficient to 'reproduce' the tabular model atmosphere with a discrepancy of less than two percent, and simultaneously yield closed form integrable equations for the variation of the elements.

Table I provides a compilation of an estimated versus a standard model atmosphere. The estimated densities given in column 3 were obtained via equation (7). The standard model atmosphere given in column 2 was obtained by using an algorithm which generated as closely as possible specific tables given in Reference 7. The standard model atmosphere used here closely resembles the Spring-Fall model with an Exospheric Temperature of 1100° Kelvin. The first column of the table is given in kilometers, and the remaining three columns are given in grams per cubic kilometer.

IV. SOLUTION OF VARIATIONAL EQUATIONS

In light of the analysis done in Section III above, we now return to the variational equations (4). If we now combine the radical terms in (4), we obtain a set of expressions containing the forms $(1 \pm \chi)^n$, and $(1 \pm \chi)^{-n}$, where $n = 1/2$ and $\chi = e^2 \cos^2 E$. If one assumes that χ will never get too large, that is, for drag satellites, e will not be larger than 0.2, then the above terms can be expanded as

$$(1 \pm \chi)^n = 1 \pm n\chi + \frac{n(n-1)}{2} \chi^2,$$

and

$$(1 \pm \chi)^{-n} = 1 \mp n\chi + \frac{n(n+1)}{2} \chi^2. \tag{10}$$

Adopting expression (6) for atmospheric density variation, the variational equations are then reduced to solving a set of indefinite integrals of the form

$$k_i \int_{E_1}^{E_2} \exp\{-(x/H_L)(\cos E_L - \cos E)\} \cos^{\ell} E \sin^p E \, dE \tag{11}$$

where k_i is simply the constant coefficient of each corresponding integral. If, on the other hand, the eccentricity is somewhat larger than normal, say around 0.5 or so, then it will be necessary to include several more terms in the expansion (10) above. This however is an algebraic problem, and computationally speaking has only the effect of changing the overall coefficients, $\{k_i\}$, in the final algorithm. The integrals are still of the form (11) above. Utilizing the fitting described in section II, the exponential of the density can now be represented as

$$b_1(E) \exp[b_2(E) \cdot E]$$

in which $b_1(E)$ and $b_2(E)$ are determined for one or several segments within an orbital revolution. Results indicate that $b_1(E)$ and $b_2(E)$ remain fixed for a considerable length of the satellite's lifetime. Refitting becomes necessary only when a and e change appreciably. This is found to occur more frequently near the end of the satellite's lifetime. In any event, the fitting procedure is instantaneous, and the calculation proceeds without interruption.

If in the drag acceleration one desires to express the density exponential so as to involve the product of J_2, the coefficient of the Earth's second zonal harmonic and the air density, one can follow the procedure of Sherrill (Reference 3) and write this term as

$$\exp\left\{-(x/H_L)\left[(1 - e\cos E) + \frac{c^2}{2a^2}\left(\frac{1-\eta^2}{1 - e\cos E}\right) + \epsilon\sigma_E\eta^2\right]\right\}$$

where $c^2 = J_2 R_e^2$. Here R_e is the value of the Earth's equatorial radius, σ_E is the equatorial radius of the oblate spheroid which passes through the initial perigee point of the satellite, and the flattening $\epsilon = 1/298$. Since this addition

is accounted for rather simply by the fitting procedure, the cross term is retained in the exponential. Using these results, equation (11) is rewritten as

$$b_1(E) \int_{E_1}^{E_2} \exp[b_2(E)\cdot E] \cos^{\ell} E \cdot \sin^{p} E\, dE. \tag{12}$$

Here p takes the values 0, 1, and 2. When $p = 0$, ℓ takes on all values from zero through twelve. When $p = 1$, ℓ goes from zero through eleven; and when $p = 2$, ℓ ranges from zero through ten. For the case $p = 0$, expression (12) reduces to

$$I_0^{\ell} = b_1(E) \int_{E_1}^{E_2} \exp[b_2(E)\cdot E] \cos^{\ell} E \; dE \; .$$

When ℓ is even ($\ell = 2n$), this becomes

$$I_0^{2n} = \frac{b_1(E)}{2^{2n}} \left[\frac{(2n)!}{(n!)^2 b_2(E)} \exp[b_2(E)\cdot E] \right. \tag{13}$$

$$\left. + 2\exp[b_2(E)\cdot E] \sum_{j=0}^{n-1} \frac{(2n)!}{(2n-j)!\,j!} \frac{b_2(E)\cos(2n-2j)E + (2n-2j)\sin(2n-2j)E}{b_2^2(E) + (2n-2j)^2} \right]_{E_1}^{E_2}$$

When ℓ is odd ($\ell = 2n+1$) we have

$$I_0^{2n+1} = \frac{b_1(E)}{2^n} \left[\sum_{j=0}^{n} \frac{(2n+1)!}{(2n+1-j)!\,j!} \exp[b_2(E)\cdot E] \right.$$

$$\left. \times \frac{[b_2(E)\cos(2n-2j+1)E + (2n-2j+1)\sin(2n-2j+1)E}{b_2^2(E) + (2n-2j+1)^2} \right]_{E_1}^{E_2} \tag{14}$$

For $p = 2$ expression (12) becomes

$$I_2^{\ell} = b_1(E) \int_{E_1}^{E_2} \exp[b_2(E)\cdot E] \cos^{\ell} E \sin^2 E dE$$

$$= b_1(E) \left[\int_{E_1}^{E_2} \exp[b_2(E)\cdot E] \cos^{\ell} E dE - \int_{E_1}^{E_2} \exp[b_2(E)\cdot E] \cos^{\ell+2} E dE \right].$$

The calculation here is identical to that for I_0^{ℓ}, with results given by equations (13) and (14) for ℓ even and odd.

Finally, for $p = 1$, we have from (12)

$$I_1^{\ell} = b_1(E) \int_{E_1}^{E_2} \exp[b_2(E)\cdot E] \cos^{\ell} E \sin E dE.$$

An integration by parts reduces this to

$$I_1^{\ell} = b_1(E) \left[\frac{-\exp[b_2(E)\cdot E] \cos^{\ell+1} E}{\ell+1} \Bigg|_{E_1}^{E_2} + \frac{b_2(E)}{\ell+1} \int_{E_1}^{E_2} \exp[b_2(E)\cdot E] \cos^{\ell+1} E dE \right].$$

Here again, the integral part of I_1^{ℓ} is given by equations (13) and (14) for the cases that $(\ell+1)$ is even or odd. Let us now define the following:

$$\kappa_0 = b_1(E)\, \rho_L (1 + b(L, U)\, a^2 e^2 \cos^2 E_L)$$

$$\kappa_1 = -2\kappa_2 \cos E_L$$

$$\kappa_2 = b_1(E)\, \rho_L\, b(L, U)\, a^2 e^2$$

$$C_1^I = 0. \quad C_2^I = 0, \quad C_3^I = 1, \quad C_4^I = 2e,$$

$$C_5^I = \frac{3}{2} e^2, \quad C_6^I = e^3, \quad C_7^I = \frac{7}{8} e^4, \quad C_8^I = \frac{3}{4} e^5,$$

$$C_9^I = \frac{11}{16}e^6, \quad C_{10}^I = \frac{5}{8}e^7, \quad C_{11}^I = \frac{5}{16}e^8, \quad C_{12}^I = 0;$$

and

$$C_1^{II} = 0, \quad C_2^{II} = 0, \quad C_3^{II} = 1, \quad C_4^{II} = 0,$$

$$C_5^{II} = -\frac{1}{2}e^2, \quad C_6^{II} = 0, \quad C_7^{II} = -\frac{e^4}{8}, \quad C_8^{II} = 0,$$

$$C_9^{II} = -\frac{e^6}{16}, \quad C_{10}^{II} = 0, \quad C_{11}^{II} = 0;$$

and

$$C_1^{III} = 0, \quad C_2^{III} = 0, \quad C_3^{III} = 1, \quad C_4^{III} = -2e,$$

$$C_5^{III} = \frac{3}{2}e^2, \quad C_6^{III} = -e^3, \quad C_7^{III} = \frac{7}{8}e^4, \quad C_8^{III} = -\frac{3}{4}e^5,$$

$$C_9^{III} = \frac{11}{16}e^6, \quad C_{10}^{III} = -\frac{5}{8}e^7, \quad C_{11}^{III} = \frac{5}{16}e^8, \quad C_{12}^{III} = 0,$$

$$C_{13}^{III} = 0;$$

and

$$C_1^{IV} = 0, \quad C_2^{IV} = 0, \quad C_3^{IV} = 1, \quad C_4^{IV} = e,$$

$$C_5^{IV} = \frac{e^2}{2}, \quad C_6^{IV} = \frac{e^3}{2}, \quad C_7^{IV} = -\frac{3}{8}e^4, \quad C_8^{IV} = \frac{3}{8}e^5,$$

$$C_9^{IV} = \frac{5}{16}e^6, \quad C_{10}^{IV} = \frac{5}{16}e^7, \quad C_{11}^{IV} = 0, \quad C_{12}^{IV} = 0;$$

and

$$C_1^V = 0, \quad C_2^V = 0, \quad C_3^V = 0, \quad C_4^V = -2e,$$

$$C_5^V = \frac{3}{2}e^2, \quad C_6^V = -e^3, \quad C_7^V = \frac{7}{8}e^4, \quad C_8^V = -\frac{3}{4}e^5,$$

$$C_9^V = \frac{11}{16}e^6, \quad C_{10}^V = \frac{5}{8}e^7, \quad C_{11}^V = \frac{5}{16}e^8, \quad C_{12}^V = 0, \quad C_{13}^V = 0;$$

and

$$C_1^{VI} = 0, \quad C_2^{VI} = 0, \quad C_3^{VI} = 1, \quad C_4^{VI} = -c,$$

$$C_5^{VI} = \frac{e^2}{2}, \quad C_6^{VI} = -\frac{e^3}{2}, \quad C_7^{VI} = -\frac{3}{8}e^4, \quad C_8^{VI} = -\frac{3}{8}e^5,$$

$$C_9^{VI} = \frac{5}{16}e^6, \quad C_{10}^{VI} = -\frac{5}{16}e^7, \quad C_{11}^{VI} = 0, \quad C_{12}^{VI} = 0.$$

Also,

$$I_1 = \sum_{\ell=0}^{10} (\kappa_2 C_{\ell+1}^{I} + \kappa_1 C_{\ell+2}^{I} + \kappa_0 C_{\ell+3}^{I})\, I_0^{\ell}$$

$$I_2 = \sum_{\ell=1}^{9} (\kappa_2 C_{\ell}^{II} + \kappa_1 C_{\ell+1}^{II} + \kappa_0 C_{\ell+2}^{II})\, I_1^{\ell},$$

$$I_3 = \sum_{\ell=0}^{9} (\kappa_2 C_{\ell+1}^{IV} + \kappa_1 C_{\ell+2}^{IV} + \kappa_0 C_{\ell+3}^{IV})\, I_1^{\ell},$$

$$I_4 = \sum_{\ell=0}^{8} (\kappa_2 C_{\ell+1}^{II} + \kappa_1 C_{\ell+2}^{II} + \kappa_0 C_{\ell+3}^{II})\, I_0^{\ell},$$

$$I_5 = \sum_{\ell=0}^{10} (\kappa_2 C_{\ell+1}^{III} + \kappa_1 C_{\ell+2}^{III} + \kappa_0 C_{\ell+3}^{III})\, I_0^{\ell},$$

$$I_6 = \sum_{\ell=0}^{9} (\kappa_2 C_{\ell+1}^{VI} + \kappa_1 C_{\ell+2}^{VI} + \kappa_0 C_{\ell+3}^{VI})\, I_1^{\ell},$$

$$I_7 = \sum_{\ell=2}^{10} (\kappa_2 C_{\ell-1}^{II} + \kappa_1 C_{\ell}^{II} + \kappa_0 C_{\ell+1}^{II})\, I_0^{\ell},$$

$$I_8 = \sum_{\ell=1}^{9} (\kappa_2 C_{\ell}^{II} + \kappa_1 C_{\ell+1}^{II} + \kappa_0 C_{\ell+2}^{II})\, I_0^{\ell},$$

$$I_9 = \sum_{\ell=1}^{10} (\kappa_2 C_\ell^{IV} + \kappa_1 C_{\ell+1}^{IV} + \kappa_0 C_{\ell+2}^{IV})\, I_0^\ell,$$

$$I_{10} = \sum_{\ell=1}^{10} (\kappa_2 C_\ell^{VI} + \kappa_1 C_{\ell+1}^{VI} + \kappa_0 C_{\ell+2}^{VI})\, I_0^\ell,$$

$$I_{11} = \sum_{\ell=0}^{10} (\kappa_2 C_{\ell+1}^{III} + \kappa_1 C_{\ell+2}^{III} + \kappa_0 C_{\ell+3}^{III})\, I_1^\ell,$$

$$I_{12} = \sum_{\ell=0}^{8} (\kappa_2 C_{\ell+1}^{II} + \kappa_1 C_{\ell+2}^{II} + \kappa_0 C_{\ell+3}^{II})\, I_1^\ell,$$

$$I_{13} = \sum_{\ell=0}^{8} (\kappa_2 C_{\ell+1}^{II} + \kappa_1 C_{\ell+2}^{II} + \kappa_0 C_{\ell+3}^{II})\, I_2^\ell,$$

$$I_{14} = \sum_{\ell=2}^{12} (\kappa_2 C_{\ell-1}^{V} + \kappa_1 C_\ell^{V} + \kappa_0 C_{\ell+1}^{V})\, I_0^\ell,$$

$$I_{15} = \sum_{\ell=1}^{11} (\kappa_2 C_\ell^{V} + \kappa_1 C_{\ell+1}^{V} + \kappa_0 C_{\ell+2}^{V})\, I_0^\ell,$$

$$I_{16} = \sum_{\ell=0}^{10} (\kappa_2 C_{\ell+1}^{III} + \kappa_1 C_{\ell+2}^{III} + \kappa_0 C_{\ell+3}^{III})\, I_2^\ell,$$

$$I_{17} = \sum_{\ell=1}^{11} (\kappa_2 C_\ell^{III} + \kappa_1 C_{\ell+1}^{III} + \kappa_0 C_{\ell+2}^{III})\, I_1^\ell.$$

Using the above quantities, we now write the solutions of the variational equation (4) as

$$\Delta a = -\frac{C_D A a^2}{m} [I_3 - 2dI_4 + d^2 I_5].$$

$$\Delta e = -\frac{1}{2}\frac{C_D A a}{m}\,[2(1-e^2)\,I_9 - d(2(1-e^2)\,I_{10} + 2e^{-1}I_8 - e(I_4 + I_7)) + d^2(2e^{-1}I_{10} - e(I_5 + I_{14}))],$$

$$\Delta S = -\frac{C_D A}{m}\,a^{5/2}\mu^{-1/2}(1-e^2)^{-1/2}\,S\sqrt{1-s}\,\operatorname{sgn}\alpha_3 \{\cos^2\beta_2(I_7 - 2I_8) + e^2\cos^2\beta_2 I_4 - 2(1-e^2)^{1/2}\sin\beta_2\cos\beta_2(I_2 - eI_{12}) + (1-e^2)\sin^2\beta_2 I_{13} - d(\cos^2\beta_2(I_{14} - 2I_{15}) + e^2\cos^2\beta_2 I_5 - 2(1-e^2)^{1/2}\sin\beta_2\cos\beta_2(I_{17} - eI_{11}) + (1-e^2)\sin^2\beta_2 I_{16})\},$$

$$\Delta\beta_3 = \frac{1}{2}\frac{C_D A}{m}\,a^{5/2}\mu^{-1/2}\omega_s(1-e^2)^{-1/2}\,\{(1-e^2)^{1/2}\cos 2\beta_2 \times (I_2 - eI_{12}) - (1-e^2)\sin\beta_2\cos\beta_2 I_{13} + \sin\beta_2\cos\beta_2(I_7 - 2I_8) + e^2\sin\beta_2\cos\beta_2 I_4 - d((1-e^2)^{1/2}\cos 2\beta_2 I_{17} - (1-e^2)\sin\beta_2\cos\beta_2 I_{16} - e(1-e^2)^{1/2}\cos 2\beta_2 I_{11} + \sin\beta_2\cos\beta_2(I_{14} - 2I_{15}) + e^2\sin\beta_2\cos\beta_2 I_5)\}, \tag{15}$$

$$\Delta\beta_2 = -\frac{1}{2}\frac{C_D A a}{m} e^{-1}(1-e^2)^{-1/2}\,[2(1-e^2)\,(I_3 - dI_6)$$

$$+ d((e^2-2)\,I_{12} + eI_2) - d^2((e^2-2)\,I_{11}$$

$$+ eI_{17}] - \sqrt{1-S}\ \operatorname{sgn}\alpha_3 \Delta\beta_3$$

and

$$\Delta\beta_1 = -\mu(-2\alpha_1)^{-3/2}\left[(1-e^2)^{1/2}\,(\Delta\beta_2 + \operatorname{sgn}\alpha_3\sqrt{1-S}\ \Delta\beta_3)\right.$$

$$\left. -\frac{C_D A a}{m}\,(I_{12} - dI_{11})\right] + \frac{3}{2}\frac{\Delta a}{a}\,(t_0 + \beta_1).$$

V. RESULTS

In order to test the BMW theory, two heavy air drag satellites with somewhat dissimilar characteristics are considered. These are the Italian San Marco-2 and the U.S. Air Force Cannonball (OAR-901). Data on these spacecrafts is as follows:

San Marco-2:

Mass m = 129.27383 kgm.

Projected Area A = 3425.3397 cm^2.

Drag Coefficient C_D = 2.1

Initial epoch: April 26, 1967, 10 hours, 12 minutes.

Initial conditions (Inertial Cartesian):

$x = +0.58725272$, $\dot{x} = -0.82890608$

$y = +0.84923499$, $\dot{y} = +0.56396878$

$z = -0.05068537$, $\dot{z} = +0.01219124$

Here, x, y, and z are in units of earth radii (6378.166 kilometers), and $\dot{x}$, $\dot{y}$, and $\dot{z}$ in units of earth radii per canonical unit of time (806.812 seconds).

Apogee height = 736.00 kilometers

Perigee height = 205.60 kilometers

Eccentricity = 0.0387

Inclination = 2.87 degrees.

Cannonball:

Mass m = 362.87392 kgm.

Projected Area A = 3423.6195 cm^2.

Drag Coefficient $C_D = 2.1$

Initial Epoch: August 7, 1971, 0 hours, 20 minutes.

Initial Conditions (Inertial Cartesian):

$x = -0.9428339$, $\dot{x} = -0.26977565$

$y = -0.28161629$, $\dot{y} = -0.40945775$

$z = +0.28038380$, $\dot{z} = -1.0092100$

Apogee height = 1957.20 kilometers

Perigee height = 130.16 kilometers

Eccentricity = 0.1230

Inclination = 92.00 degrees.

In both cases, the boundary values of the atmospheric density profile given by ρ_L are taken from a static model, namely, the 1966 U. S. Standard Air Force Supplements. The profiles used here include a Spring-Fall model with an 1100 degree exospheric temperature, a Winter, 800 degree model, and a Summer 1000 degree model. While these profiles are adequate if chosen carefully, it is felt that a somewhat more sophisticated and dynamic model such as given by Jacchia (Reference 8) would not only improve results but also make them more reliable.

Figure 1, shows the variation over one orbital period (from time of insertion) of the semi-major axis, eccentricity, and $(\beta_2 + \beta_3)$ respectively for San Marco-2. Here, a_0 and e_0 are taken to be the initial values of these parameters. For the semi major axis, we have initially a secular decrease of 108 parts in 10^6 per revolution, with a periodic variation superimposed, of about 25 parts in 10^6 with the orbital period. The eccentricity shows a secular decrease of approximately 97 parts in 10^6 per revolution, and a periodic variation superimposed on it with an amplitude of about 22×10^{-6}, with the orbital period. Figure 1 shows that $(\beta_2 + \beta_3)$ shifts back and forth by about 8.3 seconds. Figure 2 is a similar graph for Cannonball. It is seen that the variations for a and e here are somewhat larger than for San Marco-2 while the shift of $(\beta_2 + \beta_3)$ is considerably less. This behavior is what one would expect considering the differences in the orbits.

Figures 3 and 4 are graphs of semi-major axis versus time (days from insertion), for San Marco-2 and Cannonball during an actual lifetime study for the two satellites. The circles are those values of a, predicted by the BMW theory using only the initial conditions given above, while the crosses indicate those arcs of data supplied by orbit improvement routines utilizing tracking or observational data to update the orbital elements. The orbital improvements were necessitated by the rapid deterioration of the orbital parameter quality due to inaccurate force modeling (particularly air resistance accelerations) in the equations of motion. The accepted date of re-entry into the earth's atmosphere for San Marco-2 was on October 14, 1967 at approximately 13 hours. Thus, the total lifetime was about 171 days. The BMW program computed a lifetime of 165 days, for a re-entry on October 8, 1967. Cannonball's re-entry date was approximately January 28, 1972, a lifetime of about 173 days. BMW computed 170 days. In these two cases, the program evaluated the limits of the variational equations for values of the eccentric anomaly corresponding to five day intervals. This was done so as to allow the BMW program to compare at intermediate points, its values for semi-major axis with the observed ones. In actual practice, these limits would be evaluated for those values of eccentric anomaly corresponding to those regions of an orbit over which a fit of the density variation remained fixed. Using a change in perigee height criterion (preselected at 1 km), results from Cannonball show that the first region is the first 65 days, the second is the next 55 days, and so on, until within the last month of life the regions

are only of 5 day durations. As a result, the entire ephemeris is computed rapidly. Using the IBM 360/91 electronic digital computer, the complete San Marco-2 and Cannonball ephemerides computed at 5 day intervals were executed in less than 18 seconds of computer CPU time.

These results show that the BMW program was within 4 percent of the "true" lifetimes of both satellites, despite the fact that Cannonball had a relatively high eccentricity and low perigee. In addition, it must be pointed out that the initial conditions used in the program were obtained from orbit improvement routines other than the Vinti Orbit Determination System, since this was the only data available. To be more consistent, and to improve accuracy, one should utilize, if possible, only those initial or epoch values obtained from the Vinti Orbit Determination System (Reference 9, 10).

In spite of the startling success with San Marco-2 and Cannonball, improvements to the present BMW computer program are being considered. Prime among these is the incorporation of a dynamic model atmospheric density profile such as Jacchia's. As is well known a slight miscalculation in the exospheric temperature for a static model would drastically alter the resulting density profile, and consequently, the computed ephemeris of the satellite.

The distinct advantage of the BMW method over numerical integration techniques is that being analytic or closed form, it is not subject to large error accumulation due to roundoff and truncation. In addition, an entire ephemeris can be obtained in a matter of a few seconds on present generation computers, while such a task might be prohibitive with a numerical integration.

With the atmospheric profile given by (5), expression (11) with p = 0 could be expressed in terms of Bessel functions; for example,

$$\frac{1}{\pi}\int_0^{\pi} \exp(c\cos E)\cos^n E\,dE = J_0(c) \qquad (n = 0)$$

$$= J_1(c) \qquad (n = 1)$$

$$= J_0(c) - \frac{1}{c} J_1(c) \qquad (n = 2)$$

and so forth. The disadvantage here, besides the limited step size over which to perform the summation, is in the difficulty of handling intermediate points within the limits. A Bessel function approach would appear to be better employed in a study of atmospheric density inference from calculations of the period decrement.

King-Hele (Reference 6) has studied the contraction of orbits in a closed form manner. Four situations are considered:

1. Normal e, Phase 1: approx. $0.02 < e < 0.2$ ($3 < (ae/H_p) < 30$ approx.)
2. Normal e, Phase 2: $0 < e < 0.02$ approx. ($0 < (ae/H_p) < 3$)
3. Circular orbits: $e = 0$ ($ae/H_p = 0$).
4. High eccentricity: $e \geq 0.2$ ($ae/H_p \geq 30$ approx.).

It is felt that the regions covered by the equations of motion in these four cases are also covered by the BMW theory. Even though a static model atmosphere profile was used in the calculations, BMW does have the latitude of utilizing a

density profile such as the Jacchia model. In addition, the reference orbit is not an exact ellipse, but the Vinti orbit. As a result, it is felt that the BMW method has contributed to the program for calculating both accurately and rapidly, the orbits of satellites experiencing aerodynamic drag.

At the present time, the Vinti differential correction algorithm (Reference 10) employing a classical weighted least squares technique is being appropriately modified to accommodate the augmented force model. The bulk of the implementation requires the reformulation of the partial derivatives $\{\partial y_i / \partial q_j(t_0)\}$ to reflect air drag where $\{y_i\}$ are tracking observables and $\{q_j(t_0)\}$ are the set of "epoch" Vinti orbital elements and an atmospheric parameter iteratively estimated by the differential correction technique. It appears that complete analyticity can be retained for these partial derivative expressions, thus merging the theoretical developments presented here with the practical application of orbit estimation. This work will be forthcoming in a future report.

ACKNOWLEDGMENTS

The authors are grateful to Dr. John P. Vinti of the Measurement Systems Laboratory, Massachusetts Institute of Technology, Cambridge, Massachusetts, and to Dr. A. Deprit of the Dept. of Astronomy, of the University of Cincinnati, for valuable discussions which contributed to this report. Also to Mr. E. M. Jones and Mr. R. A. Gordon of the Goddard Space Flight Center for their assistance with some of the numerical calculations of this report.

REFERENCES

1. Vinti, John P., "Gaussian Variational Equations for Osculating Elements of an Arbitrary Separable Reference Orbit," Celestial Mechanics Journal, I, No. 3, pp. 367-375, 1973.
2. Brouwer, D. and G. Hori, "Theoretical Evaluation of Atmospheric Drag Effects in the Motion of an Artificial Satellite," Astronomical J., 66, No. 2, p. 39, 1961.
3. Sherrill, J. J., "Development of a Satellite Drag Theory Based on the Vinti Formulation," (Ph. D. Dissertation), Univ. of California, Berkeley, 1966.
4. Vinti, John P., "Improvement of the Spheroidal Method for Artificial Satellites," Astronomical J., 74, No. 1, pp. 25-34, 1969.
5. Sterne, T. E., "An Introduction to Celestial Mechanics," Interscience Publishers, Inc., New York, 1960.
6. King-Hele, Desmond, "Theory of Satellite Orbits in an Atmosphere," Butterworth and Co. (Publishers) LTD., London, 1964.
7. U. S. Standard Atmosphere Supplements, 1966, (ESSA, NASA, USAF), U. S. Government Printing Office, Washington, D. C.
8. Roberts, C. E., "An Analytic Model for Upper Atmosphere Densities Based upon Jacchia's 1970 Models," Celestial Mechanics Journal, 4, pp. 368-377, 1971.
9. Bonavito, N. L., "Computational Procedure for Vinti's Accurate Reference Orbit with Inclusion of the Third Zonal Harmonic," NASA TN D-3562, August 1966.
10. Walden, H. and J. S. Watson, "Differential Corrections Applied to Vinti's Accurate Reference Orbit with Inclusion of the Third Zonal Harmonic," NASA TN D-4088, August 1967.

TABLE I

Height	Static ATM Density	RHO	DIFF.
0.2050000000000D 03	0.301060802633D 03	0.301060802633D 03	0.0
0.2060000000000D 03	0.292581857391D 03	0.292581857391D 03	0.113686837722D-12
0.2070000000000D 03	0.284373995477D 03	0.284373956992D 03	0.384845234862D-04
0.2080000000000D 03	0.276427541284D 03	0.276427541284D 03	0.113686837722D-12
0.2090000000000D 03	0.268733199909D 03	0.268733129768D 03	0.701411933051D-04
0.2100000000000D 03	0.261282040805D 03	0.261281906415D 03	0.134389794596D-03
0.2110000000000D 03	0.254065482185D 03	0.254065482185D 03	0.213162820728D-13
0.2120000000000D 03	0.247075276161D 03	0.247075072937D 03	0.203224049809D-03
0.2130000000000D 03	0.240303494560D 03	0.240302827238D 03	0.667321502970D-03
0.2140000000000D 03	0.233742515394D 03	0.233741317168D 03	0.119822619084D-02
0.2150000000000D 03	0.227385009955D 03	0.227383378171D 03	0.163178351055D-02
0.2160000000000D 03	0.221223930490D 03	0.221222099643D 03	0.183084742385D-02
0.2170000000000D 03	0.215252498448D 03	0.215250815844D 03	0.168260392789D-02
0.2180000000000D 03	0.209464193246D 03	0.209463097141D 03	0.109610524396D-02
0.2190000000000D 03	0.203852741559D 03	0.203852741559D 03	0.248689957516D-13
0.2200000000000D 03	0.198412107074D 03	0.198417301338D 03	-0.519426438754D-02
0.2210000000000D 03	0.193136480719D 03	0.193156793127D 03	-0.203124082286D-01
0.2220000000000D 03	0.188020271319D 03	0.188064945792D 03	-0.446744726403D-01
0.2230000000000D 03	0.183058096672D 03	0.183135719948D 03	-0.776232757051D-01
0.2290000000000D 03	0.156242633526D 03	0.156564335714D 03	-0.421702188640D 00
0.2330000000000D 03	0.141611890377D 03	0.141568571597D 03	0.331878055081D-02
0.2370000000000D 03	0.128303946660D 03	0.128303946660D 03	0.284217094304D-13
0.2450000000000D 03	0.105648314722D 03	0.105642771638D 03	0.554308315159D-02
0.2500000000000D 03	0.937586310738D 02	0.937487761412D 02	0.985493260362D-02
0.2700000000000D 03	0.590301268805D 02	0.590233812922D 02	0.674558833808D-02
0.2790000000000D 03	0.482902323517D 02	0.482837020943D 02	0.530257381655D-03
0.2850000000000D 03	0.423415114719D 02	0.423456469834D 02	-0.413552152309D-02
0.2930000000000D 03	0.313821645875D 02	0.314306093484D 02	-0.484447609329D-01
0.3420000000000D 03	0.134720611316D 02	0.134712758807D 02	0.785150904546D-03
0.4100000000000D 03	0.398871539430D 01	0.408449712729D 01	-0.957817329940D-01
0.4800000000000D 03	0.129181693981D 01	0.129159554315D 01	0.221396651137D-03
0.5500000000000D 03	0.449473286944D 00	0.453450297264D 00	-0.397701031921D-02
0.6500000000000D 03	0.112075750808D 00	0.112756896810D 00	-0.681146001936D-03

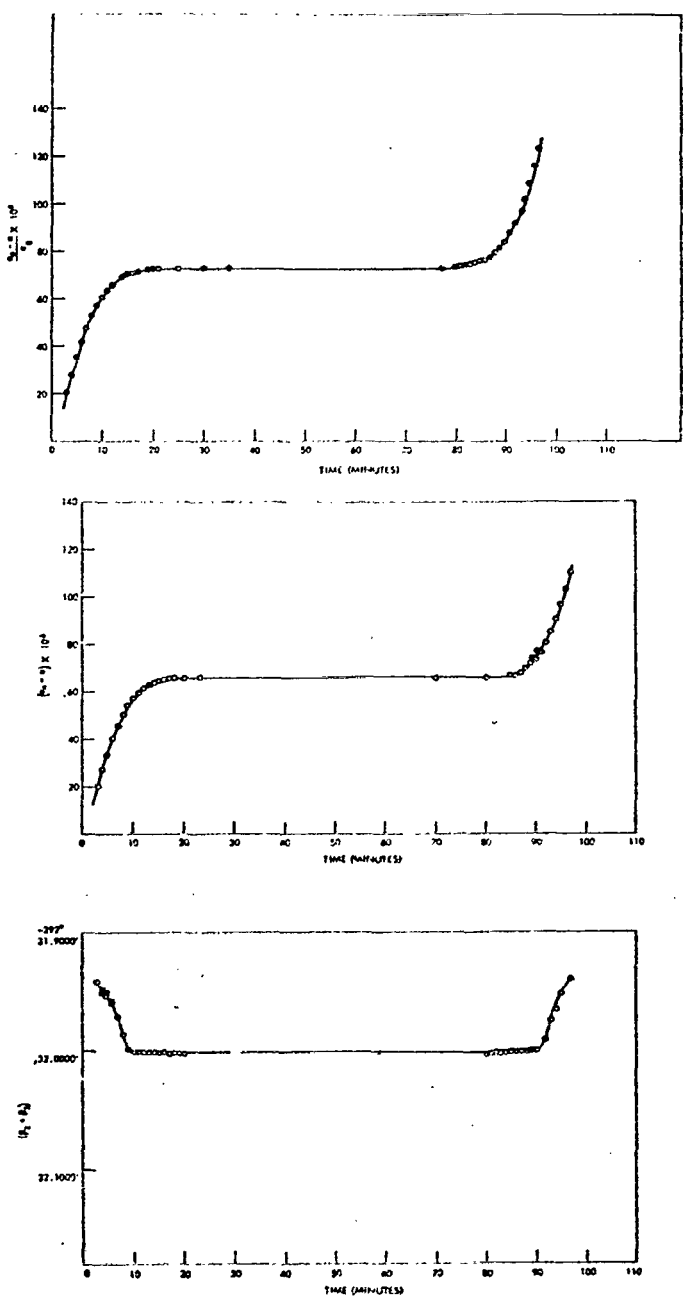

Figure 1. Variation of a, e, and $(\beta_2 + \beta_3)$ for San Marco-2

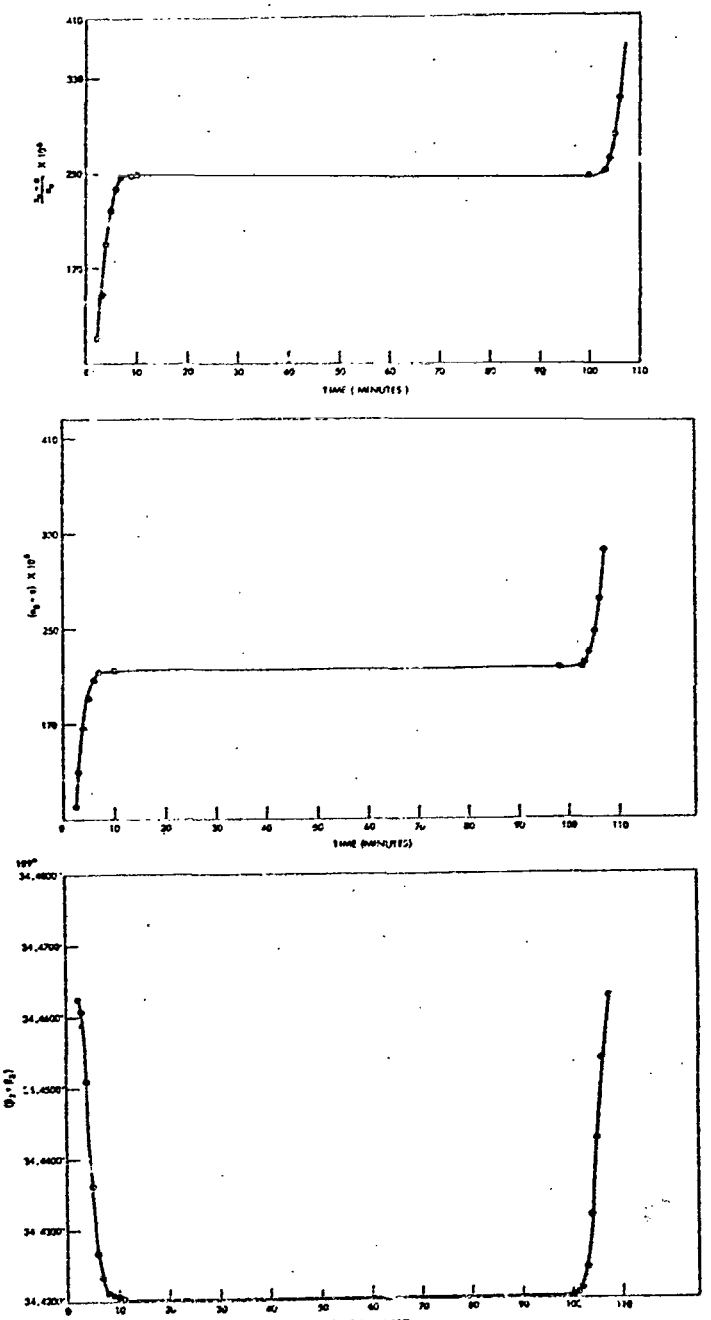

Figure 2. Variation of a, e, and $(\beta_2 + \beta_3)$ for Cannonball

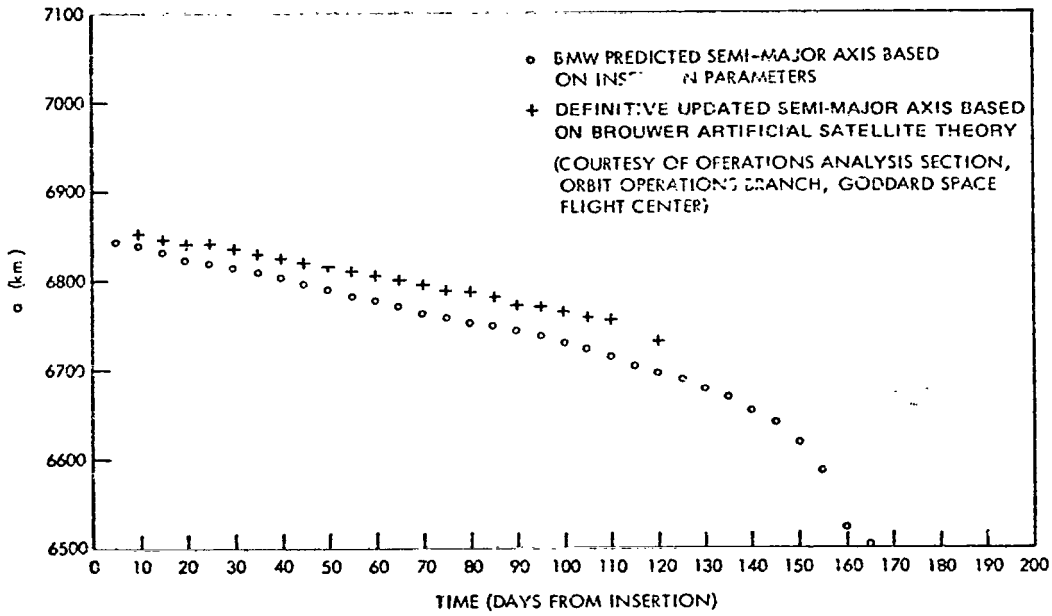

Figure 3. Variation of Semi-Major Axis for San Marco-2

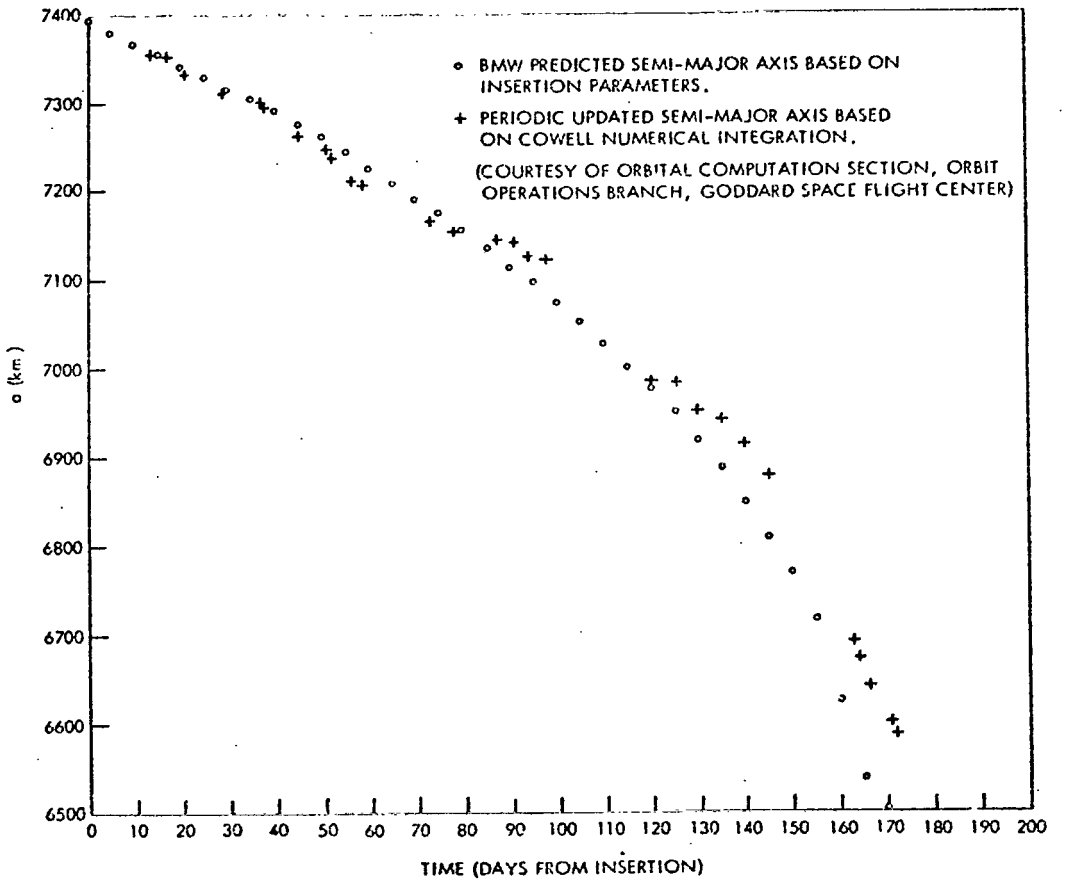

Figure 4. Variation of Semi-Major Axis for Cannonball

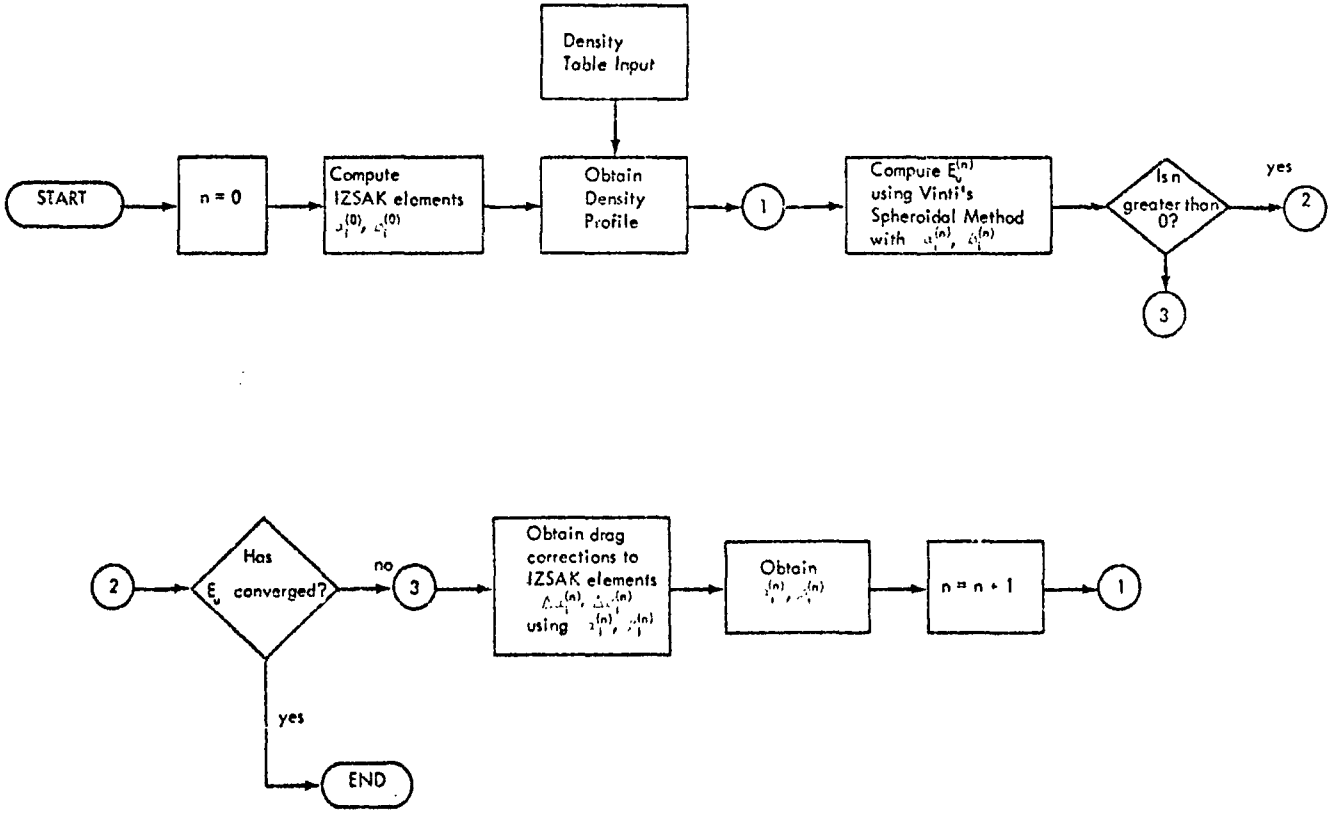

Figure 5. BMW Computational Algorithm for Drag-Oblateness Interaction

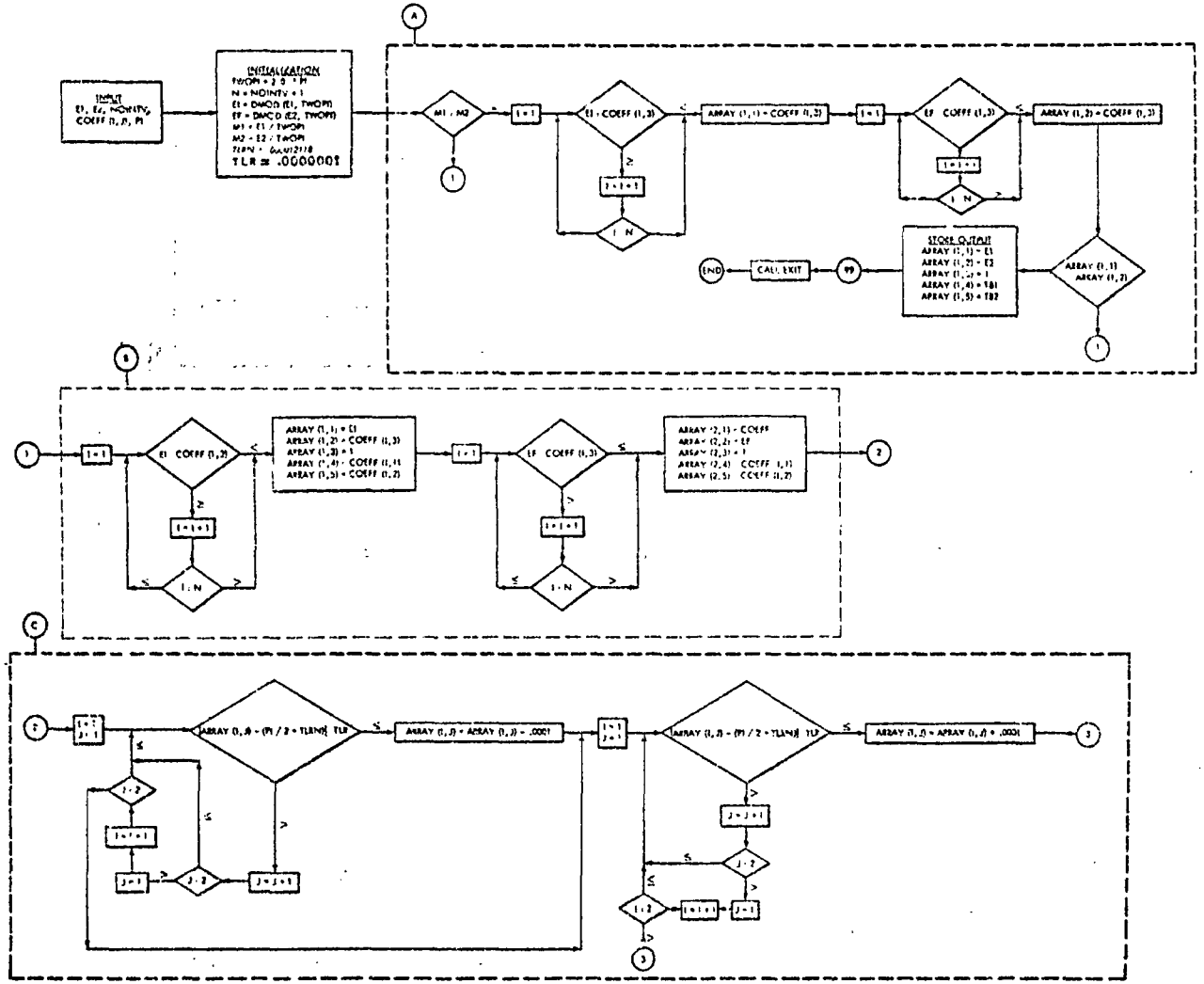
INPUT
INITIALIZATION
TLR = .0000001
STORE OUTPUT
CALL EXIT
END
99

Figure A-1

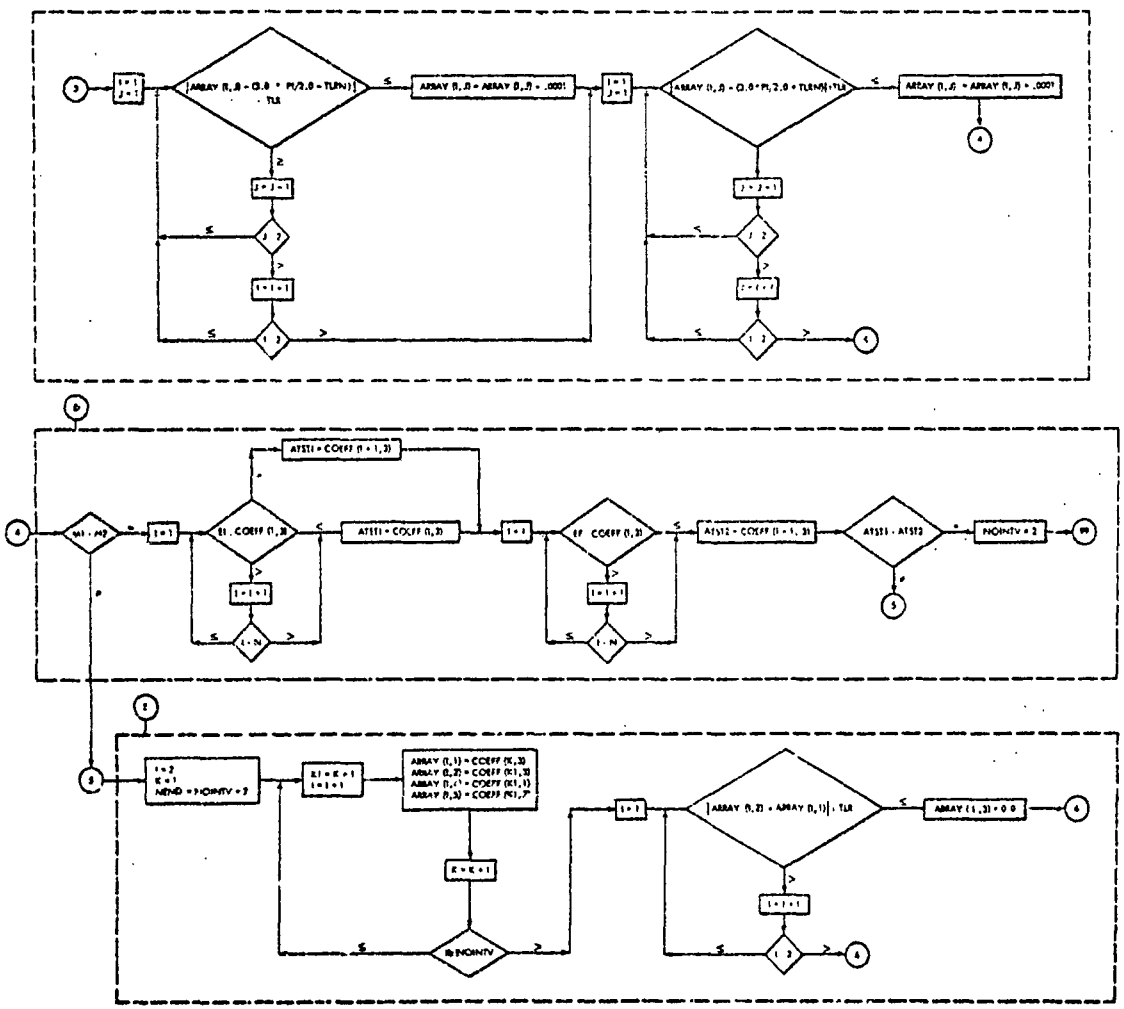

Figure A-1 (continued)

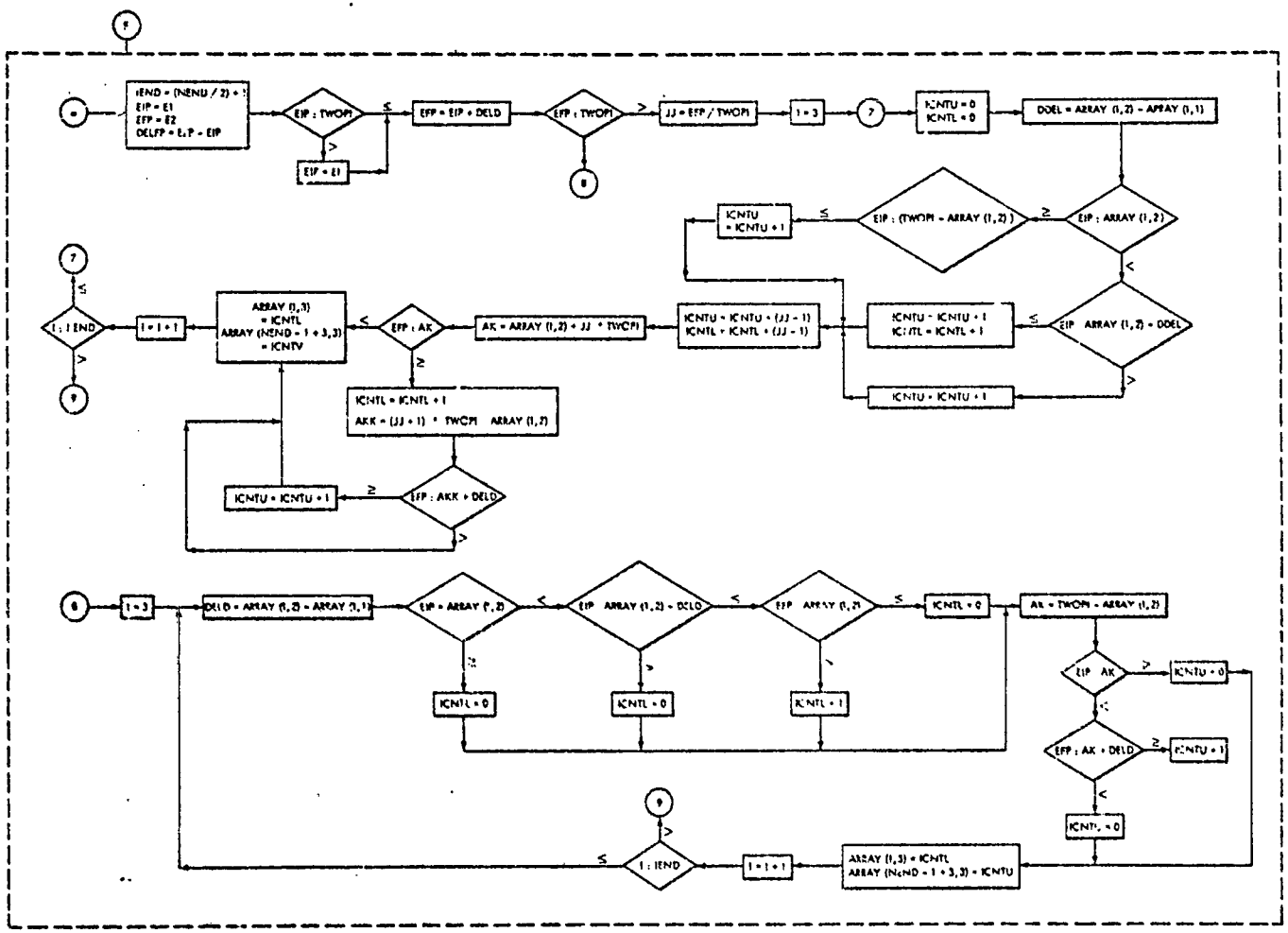

Figure A-1 (continued)

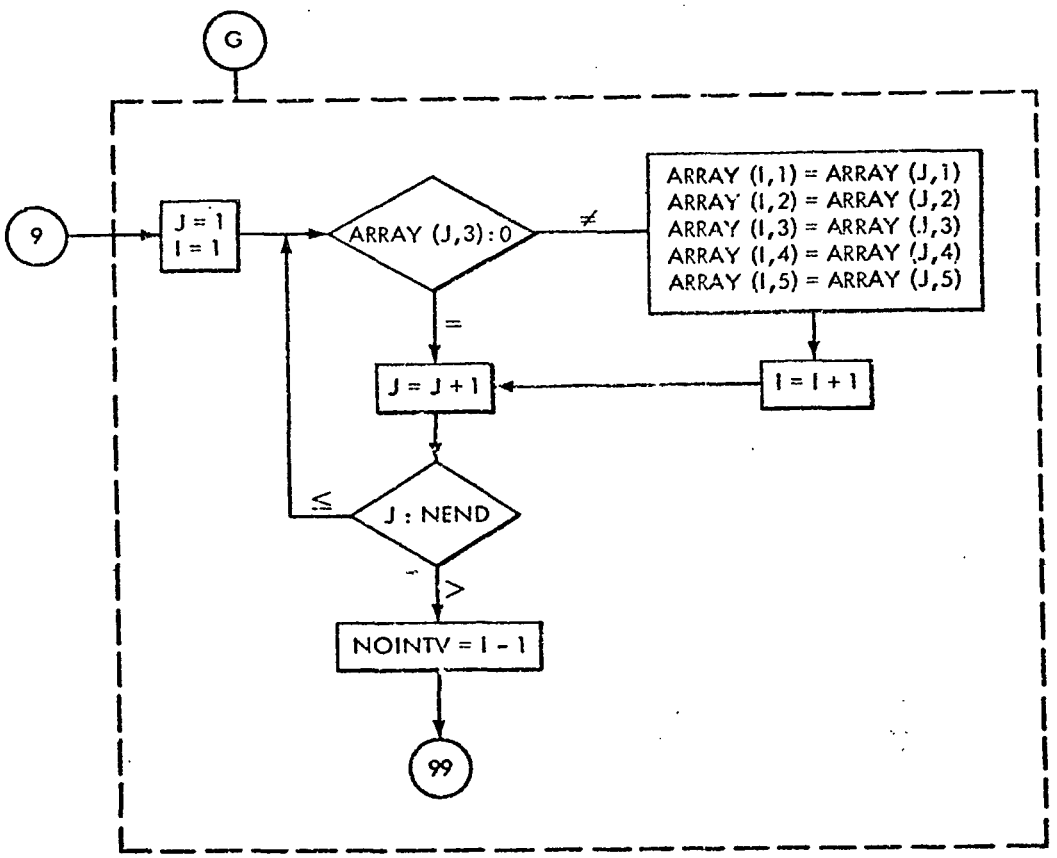

Figure A-1 (continued)

APPENDIX

DEVELOPMENT OF VARIATIONAL EQUATION CONSTANTS

For $k = 1, 2, \ldots, 6$; the general expression for the change in the Vinti orbital elements due to atmospheric drag between the arbitrary limits E_1^*, E_2^* is given by:

$$\begin{aligned}\Delta q_k = &\sum_{j=0}^{n-1} m_{j+1} \int_{x_j}^{x_{j+1}} \{t_{j+1} \exp [d_{j+1} E]\} \, dG_k(E) \\ &+ \sum_{j=0}^{n-1} m_{2n-j} \int_{2\pi - x_{j+1}}^{2\pi - x_j} \{t'_{2n-j} \exp [d'_{2n-j} E]\} \, dG_k(E) \\ &+ \int_{x_\xi}^{E_2^* \bmod 2\pi} t_\xi^* \exp [d_\xi^* E] \, dG_k(E) \\ &+ \int_{E_1^* \bmod 2\pi}^{x_\eta} t_\eta^* \exp [d_\eta^* E] \, dG_k(E)\end{aligned} \tag{A-1}$$

Without loss of generality, assume that the fitting process is performed over the interval $[0, \pi]$ i.e.

$$0 = x_0 < x_1 < x_2 < \cdots < x_{n-1} < x_n = \pi,$$

the coefficients t_ℓ are expressed by

$$t_\ell = c_\ell \left[1 + b(L, U)\, x^2 (\cos E_L - \cos E)^2\right] \quad (\ell = 1, 2 \cdots n) \tag{A-2}$$

where c_ℓ is a previously defined fitted parameter in the interval $I_\ell[x_{\ell-1}, x_\ell]$ $\ell = 1, 2, \ldots n$; $x = ae$. From symmetry considerations define

$$x_{2n-\ell} = 2\pi - x_\ell \tag{A-3}$$

$$I_{2n-\ell+1} = (2\pi - x_\ell,\ 2\pi - x_{\ell-1}) \tag{A-4}$$

$$t'_{2n-\ell+1} = c_\ell \exp(2\pi d_\ell)\left[1 + b(L, U)\, x^2 (\cos E_L - \cos E)^2\right] \quad \ell = 1, 2, \ldots n \tag{A-5}$$

$$d'_{2n-\ell+1} = -d_\ell \tag{A-6}$$

$$c'_{2n-\ell+1} = c_\ell \tag{A-7}$$

where d_ℓ is the other previously defined, subinterval dependent, fitted parameter.

The remainder of this appendix shows the procedure utilized to derive the values of the non negative integer multiplicity factors m_ℓ, $m_{n+\ell}$ $\ell = 1, 2, \ldots n$; the value ξ, an integer between 0, 2n - 2; the value of η, an integer between 1, 2n - 1; and (t^*_ξ, t^*_η) which may be (t_ξ, t_η), (t'_ξ, t_η), (t_ξ, t'_η), or (t'_ξ, t'_η) depending upon whether E_1^* mod 2π and E_2^* mod 2π are less than or equal to or greater than π, for arbitrary E_1^*, E_2^* and for different modes of operation of the orbit

program. Prior to defining this procedure, consider the following definitions concerning (A) modes of operation of the Vinti orbit generator program, (B) integration intervals of the variational equations, and (C) Fortran variable definitions.

(A) Mode I

The Vinti orbit generator program is operating in mode I when the time span of the variational equation integration [or implicitly, the integration interval (E_1^*, E_2^*)] is sufficiently small so that there is not a complete fitting subinterval imbedded between the integration limits. Mode I will be the dominant mode for definitive ephemerides or an ephemeris computed to support a differential correction.

Mode II

The Vinti orbit generator is operating in mode II when the time span of variational integration has one or more imbedded fitting subintervals between the limits of variational equation integration. This mode will be utilized in lifetime studies when large intervals of integration will be performed. Note that mode II implies the assumption of a valid fit (or x = ae constant) over large periods of time than does mode I where new fits will be performed as frequently as is required.

(B) Class I Interval

A class I interval is an interval such that both boundary points are adjacent grid points of the mesh $x_0, x_1, \ldots, x_n$.

Class II Interval

A class II interval is an interval such that one boundary point of the interval is a point x_j of the mesh $x_0, x_1, \ldots, x_n$ while the other boundary point is a non mesh point between

$$x_j \text{ and } x_{j+1}.$$

(C) Fortran Variable Definitions

Fortran Variables	Mathematical Description
E1	E_1^*
E2	E_2^*
NOINTV	$2n$

$$\text{COEFF}(I,J)\ J=1 \begin{cases} I = 2, \dfrac{\text{NOINTV}}{2}+1 & c_1 \text{ to } c_n \\ I = \begin{cases} \dfrac{\text{NOINTV}}{2}+2, & c_{n+1} \text{ to } c_{2n} \\ \text{NOINTV}+1 \end{cases} \end{cases}$$

$$J=2 \begin{cases} I = 2, \dfrac{\text{NOINTV}}{2}+1 & d_1 \text{ to } d_n \\ I = \begin{cases} \dfrac{\text{NOINTV}}{2}+2, & d'_{n+1} \text{ to } d'_{2n} \\ \text{NOINTV}+1 \end{cases} \end{cases}$$

$$J=3 \quad \{I = 1, \text{NOINTV}+1 \qquad x_0, x_1, \cdots x_{2n}$$

ARRAY (I, J)

$$I = 1 \begin{cases} J = 1 & E_1^* \bmod 2\pi \\ J = 2 & x_\eta \\ J = 3 & 0 \text{ or } 1 \\ J = 4 & t^*_\eta \\ J = 5 & d^*_\eta \end{cases}$$

$$I = 2 \begin{cases} J = 1 & x_\xi \\ J = 2 & E_2^* \bmod 2\pi \\ J = 3 & 0 \text{ or } 1 \\ J = 4 & t^*_\xi \\ J = 5 & d^*_\xi \end{cases}$$

$$I = 3, \text{NOINTV} + 2 \begin{cases} J = 1 & x_0, x_1, \cdots, x_{2n-1} \\ J = 2 & x_1, x_2, \cdots, x_{2n} \end{cases}$$

$$I = 3, \frac{\text{NOINTV}}{2} + 1 \begin{cases} J = 3 & m_\ell \\ J = 4 & c_\ell \\ J = 5 & d_\ell \end{cases}$$

$$I = \frac{\text{NOINTV}}{2} + 2, \text{NOINTV} + 2 \begin{cases} J = 3 & m_{n+\ell} \\ J = 4 & c'_{n+\ell} \\ J = 5 & d'_{n+\ell} \end{cases}$$

The following describes the subtasks associated with defining the full set of integration parameters in (A-1). The detailed logic is presented in the flow-chart given in Figure A-1.

Ⓐ This algorithm will test whether E_1^* and E_2^* are within the same subinterval, will store the proper interval of integration and associated constants into ARRAY, and exit. This simplified logic is most useful in Mode I orbit generations.

Ⓑ This algorithm defines the Class II intervals associated with the arbitrary limits E_1^*, E_2^*, (i.e. $[x_\xi, E_2^* \bmod 2\pi]$ and $[E_1^* \bmod 2\pi, x_\eta]$) and stores them and the associated constants into ARRAY.

Ⓒ This algorithm checks to see if any of the Class II intervals are near $\pi/2$ or $3\pi/2$ in order to avoid underflow difficulties during evaluation of the integrals.

Ⓓ To assist the task of deleting unnecessary computations in Mode I generations, this algorithm establishes the necessary intervals and associated constants when E_1^* and E_2^* are in adjacent subintervals and in the same multiple of 2π.

Ⓔ This logic stores the entire set of Class I subintervals and associated constants into ARRAY and checks the Class II subintervals for negligible length. If such a Class II interval is found, it is eliminated from consideration. An arbitrary interval length of 1×10^{-7} is the criterion presently used.

(F) This algorithm defines m_ℓ, $m_{n+\ell}$. It is predominantly used in Mode II orbit generations.

(G) This algorithm redefines ARRAY to eliminate Class I intervals with a multiplicity factor of zero and Class II intervals whose multiplicity factor has been reset from one to zero by (E) when its length is negligible.